

# C–H Bond Activation through $\sigma$ -Bond Metathesis and Agostic Interactions: Deactivation Pathway of a Grubbs Second-Generation Catalyst

Jomon Mathew,<sup>†</sup> Nobuaki Koga,<sup>‡</sup> and Cherumuttathu H. Suresh<sup>\*†</sup>

Computational Modeling and Simulation Section, National Institute for Interdisciplinary Science and Technology (CSIR), Trivandrum, Kerala, India, and Graduate School of Information Science, Nagoya University, Chikusa-ku, Nagoya, Japan

Received June 3, 2008

A mechanistic study has been carried out to explore the structural and energetic features leading to the decomposition pathways of a Grubbs second-generation olefin metathesis catalyst using density functional theory. The active form of the catalyst **2** has an inherent tendency to undergo intramolecular reactions, as the highly electron-deficient ruthenium center is in close proximity to the C–H bonds of the N-substituents. The theoretical results strongly suggest that the deactivation pathway initiates with the C–H activation rather than pericyclic cyclization suggested for the related Grubbs–Hoveyda catalyst system by Blechert et al. Complex **2** passes through five transition states, viz., (i) formation of an agostic complex through the activation of a C–H bond of the N-heterocyclic carbene (NHC)-phenyl ring; (ii) C–H  $\sigma$ -bond metathesis with a carbene moiety to form a benzyl complex; (iii) two-step rotational transformations of the benzyl unit; and (iv) carbene–arene bond formation to yield the first product, **3**. The last step is the rate-determining step, with the highest activation barrier of 28.6 kcal/mol, while the activation energy for steps (i), (ii), and (iii) are 13.6, 26.7, and 18.8 kcal/mol, respectively. The transformation of the rigid carbene unit to a flexible benzyl unit facilitates the rotational transformations in step (iii) and the subsequent C–C bond formation in step (iv). The  $\eta^6$ -coordination of phenyl ring in **3** changes to  $\eta^2$  to produce a less strained complex, and the C–H activation of the second NHC-phenyl ring occurs easily with this transformation, leading to a C–H agostic complex through a transition state with the activation barrier of 28.3 kcal/mol. The agostic interaction breaks up in the next step, leading to the ruthenium–carbon bond formation and the reductive elimination of HCl to the second product, **4**. The flexibility of all three phenyl rings through their single bond connectivity plays a major role in the deactivation process of **2**, as it leads to C–H agostic interactions with the ruthenium center. Therefore, the deactivation can be controlled by designing NHCs with rigid substituents, which may not undergo agostic interactions.

## Introduction

N-Heterocyclic carbenes (NHCs), introduced as an analogue to phosphines, are recently getting wide attention in the design of homogeneous catalytic systems,<sup>1–6</sup> as their powerful  $\sigma$ -donating and weak  $\pi$ -accepting ability impart major changes in the reactivity of a metal complex.<sup>6–8</sup> For instance, the high catalytic efficiency observed in the second-generation Grubbs olefin metathesis catalyst **1** (Figure 1) has been attributed to

the presence NHC ligands.<sup>9–14</sup> The role of steric and electronic effects of NHCs toward the enhanced activity of catalysts on replacing phosphines by NHCs has been proved both theoretically and experimentally.<sup>12,14–20</sup> Catalyst activity can be improved by altering the substituents on the nitrogen of NHCs, and there exist a number of modified second-generation Grubbs

\* Corresponding author. E-mail: sureshch@gmail.com.

<sup>†</sup> National Institute for Interdisciplinary Science and Technology.

<sup>‡</sup> Nagoya University.

(1) Herrmann, W. A. *Angew. Chem., Int. Ed.* **2002**, *41*, 1290–1309.

(2) Marion, N.; Navarro, O.; Mei, J.; Stevens, E. D.; Scott, N. M.; Nolan, S. P. *J. Am. Chem. Soc.* **2006**, *128*, 4101–4111.

(3) Nolan, S. P. *N-Heterocyclic Carbenes in Synthesis*; Wiley-VCH: Weinheim, 2006.

(4) Bourissou, D.; Guerret, O.; Gabbai, F. P.; Bertrand, G. *Chem. Rev.* **2000**, *100*, 39–91.

(5) Glorius, F. *N-Heterocyclic Carbenes in Transition Metal Catalysis*; Springer-Verlag: Berlin, Germany, 2007.

(6) Grubbs, R. H. *Handbook of Metathesis*; Wiley-VCH: Weinheim, Germany, 2003.

(7) Scott, N. M.; Nolan, S. P. *Eur. J. Inorg. Chem.* **2005**, *2005*, 1815–1828.

(8) Crudden, C. M.; Allen, D. P. *Coord. Chem. Rev.* **2004**, *248*, 2247–2273.

(9) Chatterjee, A. K.; Morgan, J. P.; Scholl, M.; Grubbs, R. H. *J. Am. Chem. Soc.* **2000**, *122*, 3783–3784.

(10) Garber, S. B.; Kingsbury, J. S.; Gray, B. L.; Hoveyda, A. H. *J. Am. Chem. Soc.* **2000**, *122*, 8168–8179.

(11) Huang, I.; Schanz, H.-J.; Stevens, E. D.; Nolan, S. P. *Organometallics* **1999**, *18*, 2370–2375.

(12) Bielwaski, C. W.; Grubbs, R. H. *Angew. Chem., Int. Ed.* **2000**, *39*, 2903–2906.

(13) Schwab, P.; Grubbs, R. H.; Ziller, J. W. *J. Am. Chem. Soc.* **1996**, *118*, 100–110.

(14) Scholl, M.; Ding, S.; Lee, C. W.; Grubbs, R. H. *Org. Lett.* **1999**, *1*, 953–956.

(15) Occhipinti, G. H.-R.; Bjørsvik; Jensen, V. R. *J. Am. Chem. Soc.* **2006**, *128*, 6952–6964.

(16) Scholl, M.; Trnka, T. M.; Morgan, J. P.; Grubbs, R. H. *Tetrahedron Lett.* **1999**, *40*, 2247–2250.

(17) Straub, B. F. *Angew. Chem., Int. Ed.* **2005**, *44*, 5974–5978.

(18) Straub, B. F. *Adv. Synth. Catal.* **2007**, *349*, 204–214.

(19) Correa, A.; Cavallo, L. *J. Am. Chem. Soc.* **2006**, *128*, 13352–13353.

(20) Tonner, R.; Heydenrych, G.; Frenking, G. *Chem. Asian J.* **2007**, *2*, 1555–1567.

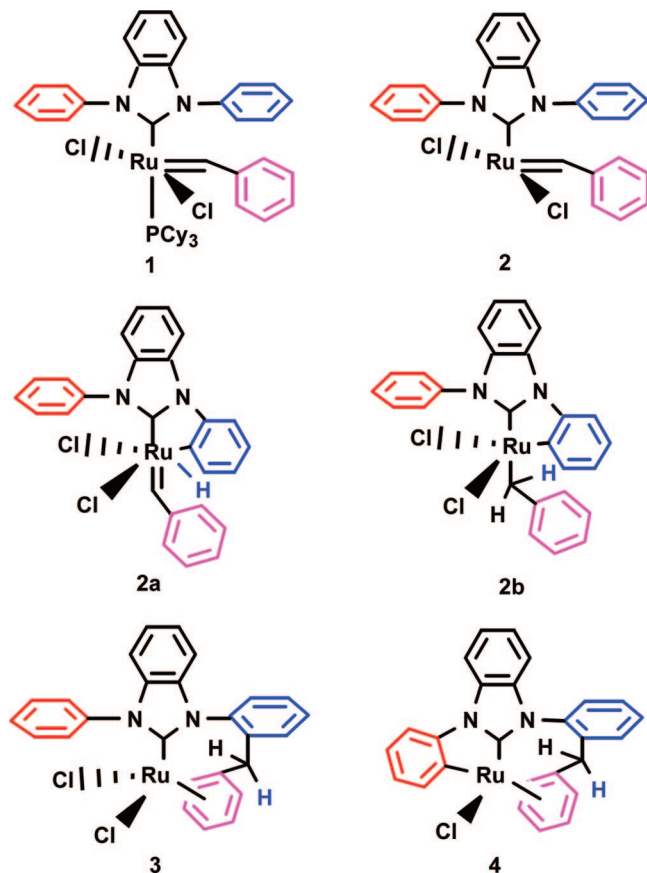


**Figure 1.** Grubbs second-generation catalyst, the proposed intermediates, and the decomposition products.

catalyst systems and even third-generation catalyst systems.<sup>12,14,21,22</sup> It has been observed that the changes in the substituents on the nitrogen on the NHC ring can change the activity of catalysts unusually in different types of metathesis reactions.<sup>14,21,22</sup>

Since olefin metathesis has emerged as an important method in organic synthesis, the designing of catalysts with suitably substituted NHCs holds great importance. However, the tendency of NHCs to undergo chemical transformations such as reductive elimination, decomplexation, and intramolecular reactions can cause the degradation of the system.<sup>8</sup> Phenyl and mesityl substituents on nitrogen were found to have a higher tendency to undergo C–H and C–C activation since the steric bulk keeps the C–H and C–C bonds close to the metal center. C–C and C–X (carbon–heteroatom) activation in ruthenium–NHC complexes were reported by Whittlesey et al.<sup>23–25</sup> Grubbs et al. have observed the possibilities of C–H activation in a second-generation Grubbs catalyst, leading to carbene–arene bond formation.<sup>26,27</sup> Blechert and co-workers reported the decomposition of a Grubbs–Hoveyda catalyst system, and they

proposed that the carbene–arene bond formation takes place directly through pericyclic cyclization.<sup>28</sup> C–H activation in rhodium–NHC complexes<sup>29,30</sup> and iridium–NHC complexes<sup>31,32</sup> was also reported.

The mechanism of olefin metathesis with the assistance of Grubbs catalyst **1** (cf. Figure 1) was already explored in both experimental and theoretical studies, and the generally accepted Chauvin mechanism suggests that the reaction initiates with the dissociation of phosphine, leading to the formation of the 14-electron complex **2** followed by olefin coordination and metathesis steps from a metallacyclobutane.<sup>33–44</sup> Therefore, complex **2** is the species having catalytic activity, and the original 16-electron complex will act only as the precatalyst. In other words, stability of the 14-electron species is directly related with the turnover number of the catalytic process. Since the metal center of **2** is highly electron deficient, it could undergo interaction even with  $\sigma$ -bonds in the vicinity. Thus electron-rich olefins can easily coordinate to the metal center to undergo metathesis reaction. However, in the absence of a substrate to coordinate with the metal or in the absence of enough concentration of the substrate, **2** may get deactivated either through intramolecular reactions or by the back-coordination of phosphine. In a recent article Grubbs et al.<sup>27</sup> reported such a deactivation reaction observed in complex **2** leading to formation of complexes **3** and **4**, in which new carbene–arene and Ru–C bonds were formed (cf. Figure 1).

The proposed mechanism<sup>27</sup> for the decomposition of Grubbs second-generation catalyst **1** involves the intermediacy of complex **2a**, a ruthenium hydride complex formed by the oxidative addition of a C–H bond of a phenyl ring to the metal center, and complex **2b**, which is formed by  $\alpha$ -H insertion to the benzylidene ligand (Figure 1). It is seen that all three phenyl ligand groups (red-, blue-, and pink-colored ones) in **2** are actively involved in the reaction and they undergo major changes. The present study will focus on this structural aspect and the complete mechanism of the transformations involved.

## Computational Methods

All calculations were carried out using the Gaussian 03<sup>45</sup> suite of programs. The optimizations, vibrational frequency, and zero-

(21) Love, J. A.; Morgan, J. P.; Trnka, T. M.; Grubbs, R. H. *Angew. Chem., Int. Ed.* **2002**, *41*, 4035–4037.

(22) Chatterjee, A. K.; Grubbs, R. H. *Org. Lett.* **1999**, *1*, 1751–1753.

(23) Burling, S.; Mahon, M. F.; Paine, B. M.; Whittlesey, M. K.; Williams, J. M. J. *Organometallics* **2004**, *23*, 4537–4539.

(24) Diggle, R. A.; Macgregor, S. A.; Whittlesey, M. K. *Organometallics* **2008**, *27*, 617–625.

(25) Diggle, R. A.; Kennedy, A. A.; Macgregor, S. A.; Whittlesey, M. K. *Organometallics* **2008**, *27*, 938–944.

(26) Trnka, T. M.; Morgan, J. P.; Sanford, M. S.; Wilhelm, T. E.; Scholl, M.; Choi, T.; Ding, S.; Day, M. W.; Grubbs, R. H. *J. Am. Chem. Soc.* **2003**, *125*, 2546–2558.

(27) Hong, S. H.; Chlenov, A.; Day, M. W.; Grubbs, R. H. *Angew. Chem., Int. Ed.* **2007**, *46*, 5148–5151.

(28) Vehlou, K.; Gessler, S.; Blechert, S. *Angew. Chem., Int. Ed.* **2007**, *46*, 8082–8085.

(29) Huang, J.; Stevens, E. D.; Nolan, S. P. *Organometallics* **2000**, *19*, 1194–1197.

(30) Dorta, R.; Stevens, E. D.; Nolan, S. P. *J. Am. Chem. Soc.* **2004**, *126*, 5054–5055.

(31) Prinz, M.; Grosche, M.; Herdtweck, E.; Herrmann, W. A. *Organometallics* **2000**, *19*, 1692–1694.

(32) Corberán, R.; Sanaú, M.; Peris, E. *Organometallics* **2006**, *25*, 4002–4008.

(33) Hérisson, J.-L.; Chauvin, Y. *Makromol. Chem.* **1970**, *141*, 161–176.

(34) Dias, E. L.; Nguyen, S. T.; Grubbs, R. H. *J. Am. Chem. Soc.* **1997**, *119*, 3887–3897.

(35) Hinderling, C.; Adlhart, C.; Chen, P. *Angew. Chem., Int. Ed.* **1998**, *37*, 2685–2689.

(36) Vyboishchikov, S. E.; Bühl, M.; Thiel, W. *Chem.–Eur. J.* **2002**, *8*, 3962–3975.

(37) Aagaard, O. M.; Meier, R. J.; Buda, F. *J. Am. Chem. Soc.* **1998**, *120*, 7174–7182.

(38) Fomine, S.; Vargas, S. M.; Tlenkopatchev, M. A. *Organometallics* **2003**, *22*, 93–99.

(39) Bernardi, F.; Bottoni, A.; Miscione, G. P. *Organometallics* **2003**, *22*, 940–947.

(40) Cavallo, L. *J. Am. Chem. Soc.* **2002**, *124*, 8965–8973.

(41) Adlhart, C.; Chen, P. *J. Am. Chem. Soc.* **2004**, *126*, 3496–3510.

(42) Suresh, C. H. *J. Organomet. Chem.* **2006**, *691*, 5366–5374.

(43) Suresh, C. H.; Baik, M. H. *Dalton Trans.* **2005**, 2982–2984.

(44) Suresh, C. H.; Koga, N. *Organometallics* **2004**, *23*, 76–80.

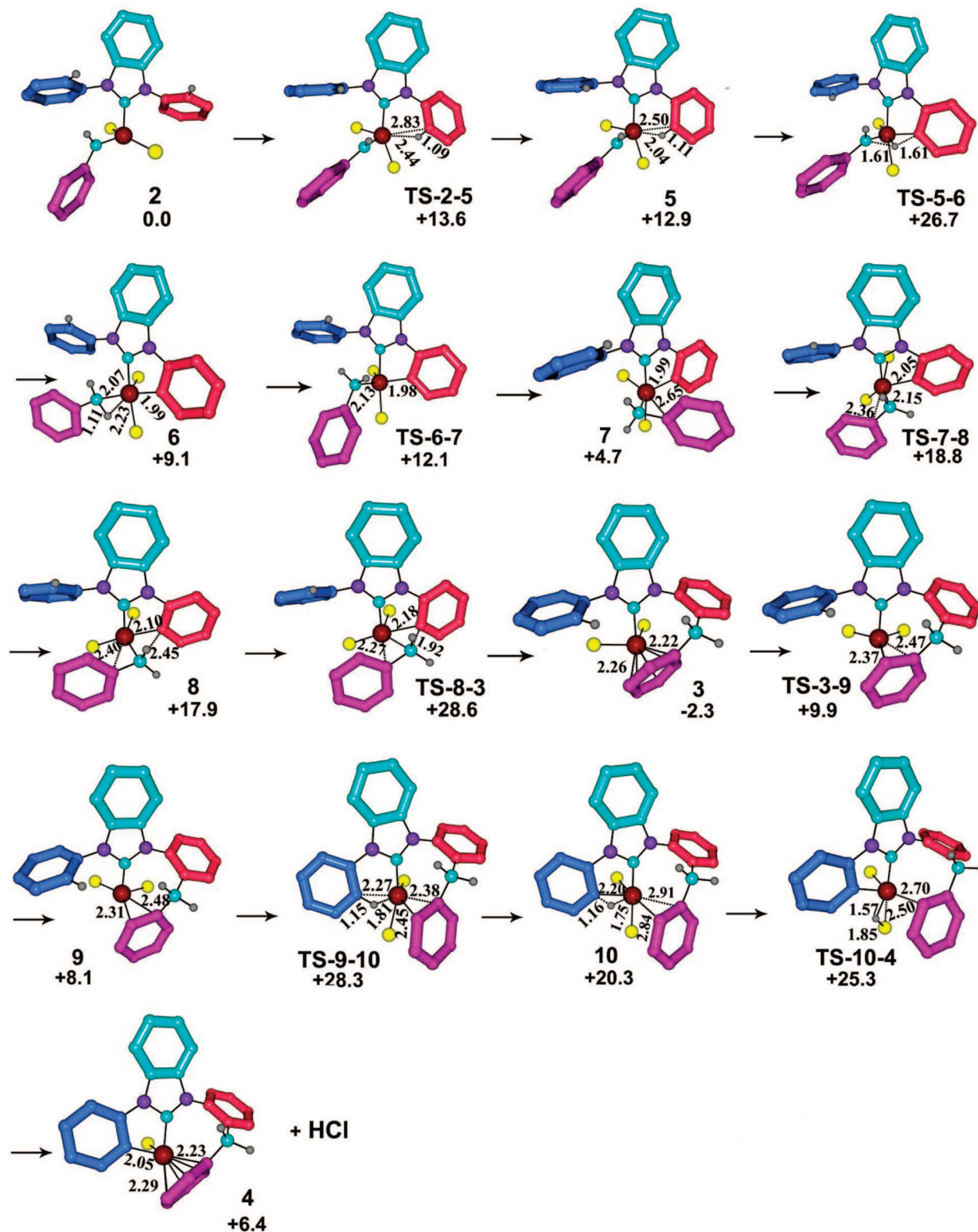


**Figure 2.** Intermediates and transition states involved in the reaction. (The relative energy values are in kcal/mol and bond lengths in Å. All nonparticipating hydrogen atoms are omitted for clarity.)

point energy (ZPE) calculations were performed using the B3LYP hybrid functional<sup>46,47</sup> and the 6-31G(d,p) basis set for all atoms except for ruthenium, which is treated with LanL2DZ with extra *f* polarization functions,<sup>48–50</sup> and the combined basis set is named Gen1. All transition states were calculated using the STQN method implemented in Gaussian 03, and transition states were characterized by a single imaginary frequency. Single-point energy calculations of all geometries were done with the B3LYP/Gen2 method, where Gen2 stands for LanL2DZ+*f* functions for Ru and 6-311++G(d,p)

for the rest of the atoms. The single-point energy values were also corrected with zero-point energy obtained from the B3LYP/Gen1 frequency calculation. The ZPE-corrected B3LYP/Gen2 level values were used throughout for discussing the energetics.

## Results and Discussion

The two probable pathways for the internal reaction to proceed from **2** can be envisaged, viz., (i) through the C–H

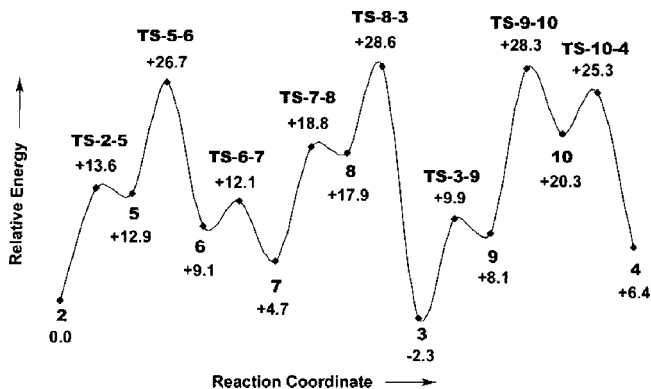


**Figure 3.** Energy profile diagram for the reaction. (The relative energy values are in kcal/mol.)

activation of the phenyl ring via agostic interactions and (ii) a pericyclic cyclization leading to a direct C–C bond formation between the carbene and arene. The intermediates and the transition states located for the first pathway are given in Figure 2 along with their important structural parameters. In Figure 3, the energetics of the reaction is plotted.

The reaction initiates with the activation of the C–H bond in the phenyl substituent on the nitrogen, leading to the formation of an agostic complex. Since two phenyl rings are present on the NHC ligand, the C–H bond of any of the phenyl rings can be activated first and the proposed mechanism<sup>27</sup> considers the C–H bond of the phenyl ring (blue) that is near the benzylidene ligand to undergo initial oxidative addition to form the ruthenium hydride complex **2a**. However, this path is not energetically favorable,<sup>51</sup> as the C–H bond of the phenyl ring that is on the opposite side of the benzylidene ligand (red) becomes activated more easily and subsequently forces the flexible phenyl ring to rotate in **TS-2-5**, leading to further reaction. The interaction of the C–H bond with ruthenium forces the C–H bond to come close to an empty d orbital of ruthenium, leading to the formation of the agostic complex **5**, where a bonding interaction exists between ruthenium and the C–H  $\sigma$ -bond. The C–H, Ru–C, and Ru–H bond lengths in complex **5** are 1.11, 1.86, and 2.50 Å, respectively, and Ru–H–C bond angle is 101°. A decrease in the Cl–Ru–Cl angle from 151° to 91° takes place during this transformation. It may be noted that the *trans* to *cis* transformation of chloro ligands in **TS-2-5** makes available a coordination site on ruthenium that is not *trans* to the strongly *trans*-influencing benzylidene ligand, so that the phenyl C–H bond easily reacts with the electron-deficient metal center to form the agostic complex **5**. In the next step, a  $\sigma$ -bond metathesis<sup>52</sup> of the agostic C–H bond takes

place in such a way that the carbon coordinates to ruthenium and H adds to the  $\alpha$ -carbon of the benzylidene ligand, leading to the formation of the complex **6**, wherein ruthenium is in the +4 oxidation state. The ruthenium hydride transition state **TS-5-6** is very similar to the intermediate **2a** in the proposed mechanism,<sup>27</sup> and the high energy associated with this transition state can be assigned to the high oxidation state of the ruthenium (Ru–H distance in **TS-5-6** is 1.65 Å). The benzyl C–H, Ru–H, and Ru–C bond lengths of 1.11, 2.23, and 2.07 Å, respectively, in **6** suggest the stabilizing agostic C–H bond interaction. Unlike the benzylidene ligand, the benzyl ligand in **6** is more flexible due to the Ru–C single bond connection, which enables the rotation of the phenyl (pink) group through **TS-6-7** to form **7**, wherein the phenyl carbon is partially coordinated to ruthenium to stabilize the complex similar to an agostic C–H bond. Subsequent rotation of the benzyl group through **TS-7-8** gives complex **8**. These internal rearrangements within the complex bring the benzyl group (pink) close to the ruthenium-coordinated phenyl (red) carbon (the C–C distance of 2.45 Å) in **8**. In addition this rearrangement makes the phenyl group (pink) interact with the central metal atom. Note that this interaction stabilizes the system and remains conserved during the subsequent reaction. A reductive elimination in **8** leads to subsequent C–C bond formation between the benzyl group and the metalated phenyl carbon to form the first product, **3**, through a four-center transition state, **TS-8-3**. In **3** the phenyl ring (pink) on the benzyl group has a  $\eta^6$ -coordination with ruthenium, where the distance between ruthenium and the center of the phenyl ring is 1.78 Å. This  $\eta^6$ -coordination makes complex **3** stable, and its relative energy value is –2.3 kcal/mol compared to **2**.

Complex **3** acts as a precursor in the formation of the second product, **4**. The  $\eta^6$ -coordinated phenyl ring changes to the  $\eta^2$ -state in **9**, and this transformation may release some ring strain associated with the methylene-bridged region (CH<sub>2</sub> between the red and pink phenyl rings) and also opens up another coordination site on the metal center. This enhances the activation of the C–H bond on the second phenyl ring (blue) and compels it to undergo rotation along the N–C  $\sigma$ -bond to form a new agostic complex, **10**, with Ru–C, Ru–H, and C–H bond lengths of 1.16, 1.75, and 2.20 Å, respectively, through the transition state **TS-9-10**. The agostic bonding observed in complex **10** is strong, as the Ru–H–C bond angle is 95.5° and the C–H bond length is 1.16 Å. This could increase the effective oxidation state of ruthenium from +2. The high energy associated with the less strained complex **10** can be attributed to the higher effective oxidation state of the metal center. Similar agostic interactions were reported by Matsubara et al. in ruthenium complexes.<sup>53,54</sup> Further activation of the agostic C–H bond to the ruthenium produces another ruthenium hydride transition state, **TS-10-4**, wherein Ru has a +4 oxidation state, and this in turn leads to the reductive elimination of HCl to form the product **4**.

(45) Frisch, M. J.; Trucks, G. W.; Schlegel, H. B.; Scuseria, G. E.; Robb, M. A.; Cheeseman, J. R.; Montgomery, J. A., Jr.; Vreven, T.; Kudin, K. N.; Burant, J. C.; Millam, J. M.; Iyengar, S. S.; Tomasi, J.; Barone, V.; Mennucci, B.; Cossi, M.; Scalmani, G.; Rega, N.; Petersson, G. A.; Nakatsuji, H.; Hada, M.; Ehara, M.; Toyota, K.; Fukuda, R.; Hasegawa, J.; Ishida, M.; Nakajima, T.; Honda, Y.; Kitao, O.; Nakai, H.; Klene, M.; Li, X.; Knox, J. E.; Hratchian, H. P.; Cross, J. B.; Bakken, V.; Adamo, C.; Jaramillo, J.; Gomperts, R.; Stratmann, R. E.; Yazyev, O.; Austin, A. J.; Cammi, R.; Pomelli, C.; Ochterski, J. W.; Ayala, P. Y.; Morokuma, K.; Voth, G. A.; Salvador, P.; Dannenberg, J. J.; Zakrzewski, V. G.; Dapprich, S.; Daniels, A. D.; Strain, M. C.; Farkas, O.; Malick, D. K.; Rabuck, A. D.; Raghavachari, K.; Foresman, J. B.; Ortiz, J. V.; Cui, Q.; Baboul, A. G.; Clifford, S.; Cioslowski, J.; Stefanov, B. B.; Liu, G.; Liashenko, A.; Piskorz, P.; Komaromi, I.; Martin, R. L.; Fox, D. J.; Keith, T.; Al-Laham, M. A.; Peng, C. Y.; Nanayakkara, A.; Challacombe, M.; Gill, P. M. W.; Johnson, B.; Chen, W.; Wong, M. W.; Gonzalez, C.; Pople, J. A. *Gaussian 03, revision C.02*; Gaussian, Inc.: Wallingford, CT, 2004.

(46) Becke, A. D. *Phys. Rev. A* **1988**, *38*, 3098–3100.

(47) Lee, C.; Yang, W.; Parr, R. G. *Phys. Rev. B* **1988**, *37*, 785–789.

(48) Hay, P. J.; Wadt, W. R. *J. Chem. Phys.* **1985**, *82*, 270–283.

(49) Hay, P. J.; Wadt, W. R. *J. Chem. Phys.* **1985**, *82*, 299–310.

(50) Ehlers, A. W.; Bohme, M.; Dapprich, S.; Gobbi, A.; Hollwarth, A.; Jonas, V.; Kohler, K. F.; Stegmann, R.; Veldkamp, A.; Frenking, G. *Chem. Phys. Lett.* **1993**, *208*, 111–114.

(51) The energy difference between complex **2** and the agostic complex **2c** (Supporting Information) formed by the rotation of the phenyl ring near the benzylidene ligand (blue) is 40 kcal/mol.

(52) Hoyt, H. M.; Michael, F. E.; Bergman, R. G. *J. Am. Chem. Soc.* **2004**, *126*, 1018–1019.

(53) Matsubara, T.; Koga, N.; Musaev, D. G.; Morokuma, K. *J. Am. Chem. Soc.* **1998**, *120*, 12692–12693.

(54) Matsubara, T.; Koga, N.; Musaev, D. G.; Morokuma, K. *Organometallics* **2000**, *19*, 2318–2329.

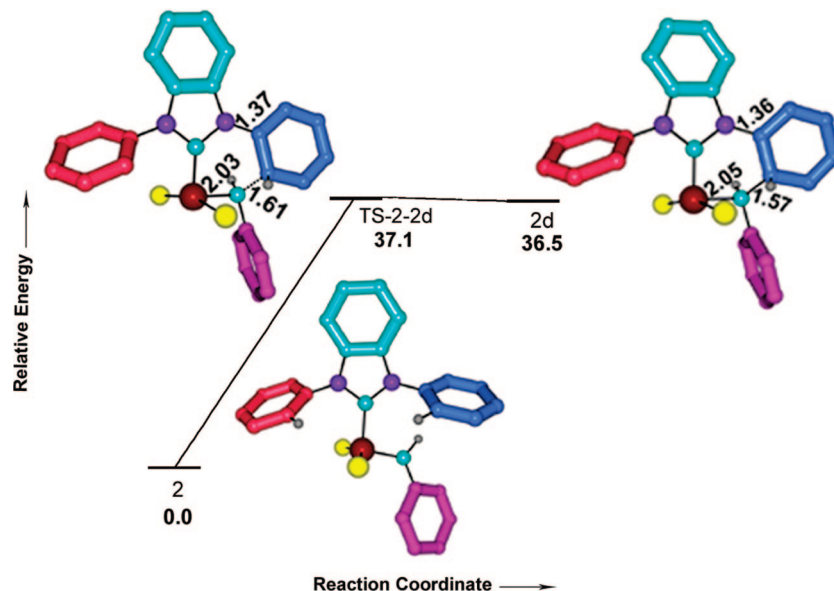


**Figure 4.** Energy profile diagram for the initial step of the pericyclic cyclization. (All bond lengths are in Å and the relative energy values are in kcal/mol. All nonparticipating hydrogen atoms are omitted for clarity.)

Although the deactivation of the active complex **2** appears to be simple in the proposed mechanism, the theoretical results suggest it is not, as it passes through five transition states to form the first product, **3**, and subsequently, **3** undergoes further reaction and forms the second product, **4**, by a three-step mechanism. The major transformations involved in the entire reaction can be summarized as (1) the formation of a C–H agostic complex with the NHC-phenyl ring, (2) C–H  $\sigma$ -bond metathesis, (3) two-step rotational transformations of the benzyl ring, (4) carbene–arene bond formation, (5) transformation of arene coordination from  $\eta^6$  to  $\eta^2$ , (6) formation of a C–H agostic complex with the second NHC-phenyl ring, (7) Ru–C bond formation, and (8) reductive elimination of HCl.

The second probable pathway for the deactivation of **2** is the pericyclic cyclization, which is a direct carbene–arene bond formation reaction at the initial stage itself. Such a mechanism was proposed for the deactivation observed in a Grubbs–Hoveyda catalyst system by Blechert et al.<sup>28</sup> The possibility of the cyclization reaction as the initial step is tested for the present case, and the relative energy values of the transition state **TS-2-2d** and the cyclic product **2d** with respect to **2** along with their structural parameters are depicted in Figure 4. The activation barrier of 37.1 kcal/mol calculated for this transformation does not support the pericyclic cyclization as the initiation step for the deactivation of **2**. Further the cyclic product **2d** is found to be stabilized only by 0.5 kcal/mol more than the transition state **TS-2-2d**, which also confirms the C–H activation as the most favorable pathway for the deactivation of **2**. In order to make a comparison of the second pathway with the deactivation reaction in the Grubbs–Hoveyda type catalyst,<sup>28</sup> we have modeled the latter at the B3LYP/GenI level. The calculated mechanism for the Grubbs–Hoveyda system was very similar to the one given in Figure 4 (energy values and structures are given in the Supporting Information). The Grubbs–Hoveyda system showed a low activation energy of 29.5 kcal/mol, which is 7.5 kcal/mol smaller than the corresponding value observed in the Grubbs system.

This decrease in the activation energy may be attributed to the chelating oxygen in the system, as it could keep the complex rigid and stable. However, the energy difference between the cyclic product and transition state is only 0.01 kcal/mol,

suggesting that the formation of the product is not feasible, as it will revert back to the original conditions. In Blechert's reaction,<sup>28</sup> the prevention of the reversibility of the reaction is claimed on the basis of subsequent oxidation in the presence of formic acid. In this reaction also the C–H bond activation pathway may be considered as another viable pathway besides the initial C–C bond formation. Elucidation of the entire mechanism of this reaction is beyond the scope of the present work.

## Conclusions

The mechanistic study presented here proves that the deactivation of the Grubbs catalyst takes place through C–H activation followed by C–H agostic interactions and  $\sigma$ -bond metathesis, and the flexibility of the phenyl groups on the N-heterocyclic carbene plays the most important role in the initiation as well as the propagation of the reaction. The C–H bonds of the flexible phenyl substituents are vulnerable for agostic bonding with the highly electron-deficient metal center, and this in turn will open up decomposition pathways of the active form of the catalyst. Further, the conversion of benzylidene to the benzyl form is also vital since this provides flexibility to the third phenyl group (pink), which otherwise would have not interacted with the metal center. Thus the results presented in this study suggest that the decomposition of the catalyst can be controlled by modifying the N-heterocyclic carbene ligand in such a way that the substituents on the nitrogen atoms have limited flexibility.

**Acknowledgment.** This research is supported by the Council of Scientific and Industrial Research (CSIR), India. J.M. thanks CSIR, India, for the financial support. Part of the computational work was carried out at Institute of Molecular Science, Okazaki, Japan, and supported by CREST, JST.

**Supporting Information Available:** Cartesian coordinates of all geometries and other details. This material is available free of charge via the Internet at <http://pubs.acs.org>.